Input Space Bifurcation Manifolds of RNNs

Robert Haschke, Jochen J. Steil

Bielefeld University, Neuroinformatics Group, Faculty of Technology
P.O.-Box 10 01 31, D-33501 Bielefeld, Germany
{rhaschke, jsteil}@techfak.uni-bielefeld.de

Abstract. We derive analytical expressions of local codim-1-bifurcations for a fully connected, additive, discrete-time RNN, where we regard the external inputs as bifurcation parameters. The complexity of the bifurcation diagrams obtained increases exponentially with the number of neurons. We show that a three-neuron cascaded network can serve as a universal oscillator, whose amplitude and frequency can be completely controlled by input parameters.

1 Introduction

An important approach to the understanding of the complex dynamical behaviour of recurrent neural networks (RNNs) is the study of their bifurcation manifolds. These manifolds separate regions in parameter space, which exhibit qualitatively different dynamical behaviour. Knowledge of these manifolds on the one hand deepens our understanding of RNNs and on the other hand allows us to directly choose parameter sets which cause a specific dynamical behaviour.

We concentrate on oscillatory behaviour of small networks, which already exhibit all kinds of dynamical behaviour and thus can serve as basic pattern generators within more complex networks, which in turn would have higher-order information processing capabilities due to resonance and synchronisation effects between its components or with respect to time-dependent inputs.

While it is commonly known, that weight parameters directly influence the dynamical behaviour of RNNs, we consider the external inputs as main bifurcation parameters and show that a three-neuron network can serve as a universal oscillator, whose amplitude and frequency – within a certain range determined by the weights – can be completely controlled with inputs.

The most simple bifurcation types are codim-1 bifurcations of fixed points, which are determined by a single bifurcation condition. Many authors have studied these bifurcation manifolds in discrete- and continuous-time neural networks before, but they employed numerical methods only and often restricted their analysis to simplified connection matrices [Beer, 1995; Pasemann, 2002; Tonnelier et al., 1999]. The first attempt to compute bifurcation manifolds of RNNs analytically was made by Hoppensteadt and Izhikevich [1997], who employed specific properties of the Fermi function

bifurcation type	eigenvalue condition	necessary test condition
saddle node	$\lambda = +1$	$\det(J(\bar{\boldsymbol{x}}) - \mathbf{1}) = 0$
period doubling	$\lambda = -1$	$\det(J(\bar{\boldsymbol{x}}) + \mathbf{1}) = 0$
Neimark-Sacker	$\lambda_{1,2} = \mathrm{e}^{\pm \mathrm{i}\omega}$ $\mathrm{e}^{\pm \mathrm{i}\omega \cdot k} \neq 1$ for $k = 1, 2, 3, 4$	$\det(J(\bar{\boldsymbol{x}}) \odot J(\bar{\boldsymbol{x}}) - \mathbf{1}) = 0$

Table 1: Test conditions for codim-1 bifurcations of discrete-time dynamical systems. $J \odot J$ is the bialternate product of matrices $J \in \mathbb{R}^{n \times n}$, also known as Kronecker product [Kuznetsov, 1995]. Its eigenvalues equal $\lambda_i \lambda_j$, $1 \leq i \leq j \leq n$.

to derive bifurcation curves of continuous-time networks. Using the same approach we already computed analytically the bifurcation curves of discrete-time two-neuron networks [Haschke et al., 2001].

The approach presented in this paper is applicable to networks of arbitrary size and with arbitrary activation, though the expressions become especially simple for the hyperbolic tangent. This extends numerical continuation techniques [Kuznetsov, 1995], which can be used to compute one-dimensional bifurcation manifolds [Beer, 1995]. Explicitly, we state the expressions for a three-neuron network. It turns out, that for more complex networks the input space is divided by so many bifurcation manifolds, that a numerical analysis and a visualisation are not feasible any more.

After the derivation of the expressions for bifurcation manifolds of saddle-node, period-doubling and Neimark-Sacker bifurcation in section 2, we compute them for a cascaded network and discuss its dynamical behaviour in section 3.

2 Derivation of Bifurcation Manifolds

We consider discrete-time recurrent neural networks

$$\boldsymbol{x} \mapsto \tanh(W\boldsymbol{x} + \boldsymbol{u}), \qquad \boldsymbol{x} \in \mathbb{R}^n \tag{1}$$

with weight matrix W and external inputs $\boldsymbol{u}$. We can restrict the activation function to the hyperbolic tangent, because it can be shown that all sigmoid activation functions within the class $\mathcal{S}_0 = \{\sigma_{\alpha,\beta,\mu}(x) = \alpha \tanh(\mu x) + \beta \,|\, \alpha, \mu \in \mathbb{R}_+, \beta \in \mathbb{R}\}$ introduced by Tiňo et al. [2001], produce topologically equivalent dynamical behaviour [Haschke, 2003]. A local codim-1-bifurcation of a fixed point is defined by the fixed point condition

$$\bar{\boldsymbol{x}} = \tanh\left(W\bar{\boldsymbol{x}} + \boldsymbol{u}\right) \tag{2}$$

and an appropriate condition on the eigenvalues of the Jacobian

$$J(\bar{\boldsymbol{x}}) = D(\bar{\boldsymbol{x}}) \cdot W \qquad \text{with} \quad D(\bar{\boldsymbol{x}}) = \mathrm{diag}\left(\tanh'(W\bar{\boldsymbol{x}} + \boldsymbol{u})\right). \tag{3}$$

All eigenvalue conditions of codim-1 fixed-point bifurcations are displayed in table 1 together with corresponding necessary test conditions, which are simpler to check. These conditions are determinant expressions involving $J(\bar{\boldsymbol{x}})$ and thus are analytical

(a) Bifurcation manifold in $\boldsymbol{\psi}$-space.

(b) Bifurcation manifold in input space.
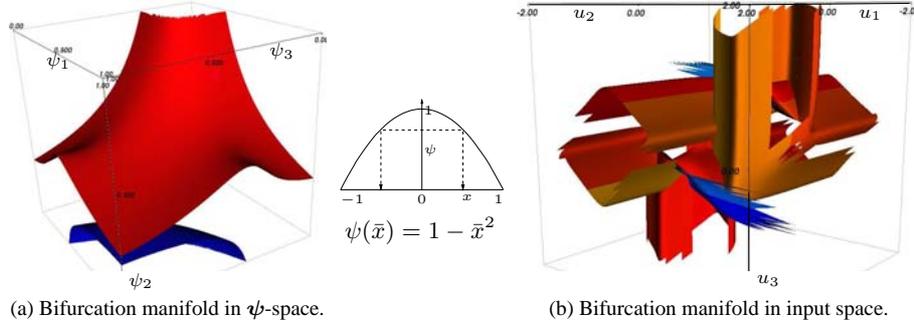
Figure 1: Neimark-Sacker bifurcation manifolds. Branches in $\boldsymbol{\psi}$-space split into 2^3 branches in input space.

$$W = \begin{pmatrix} 1.6 & 0.8 & 0 \\ -0.8 & 1.6 & 0.6 \\ 0 & -0.6 & 1.6 \end{pmatrix}$$

functions of the entries of $J(\bar{\boldsymbol{x}})$. To derive a bifurcation manifold, this system of nonlinear equations – composed of (2) and the appropriate test condition of table 1 – has to be solved for the external inputs $\boldsymbol{u} \in \mathbb{R}^n$, yielding a n-1-dimensional manifold in input space. To this end, we assume that the network's weights are constant or at least varying on a slow time scale.

The key idea is to split the solution process into two stages: First we solve the test condition within the abstract space of derivatives

$$\boldsymbol{\psi}(\bar{\boldsymbol{x}}) := \tanh'(W\bar{\boldsymbol{x}} + \boldsymbol{u}) = \mathbf{1} - \tanh^2(W\bar{\boldsymbol{x}} + \boldsymbol{u}) \overset{(2)}{=} \mathbf{1} - \bar{\boldsymbol{x}}^2 \in (0,1]^n$$

and subsequently we transfer the resulting n-1-dimensional solution manifold to input space. While this approach is applicable for networks of arbitrary size, we state the solution for three-neuron networks to simplify matters. For saddle-node and period-doubling bifurcations we obtain conditions, which are linear w.r.t. each ψ_i:

$$\det(J \mp \mathbf{1}) = \mp 1 + \sum \psi_i w_{ii} + \psi_1 \psi_2 \psi_3 \det W$$
$$\mp [\psi_1 \psi_2 \det W_{(3)} + \psi_2 \psi_3 \det W_{(1)} + \psi_1 \psi_3 \det W_{(2)}] = 0$$

$$\psi_1 = \frac{\pm 1 - \psi_2 w_{22} - \psi_3 w_{33} \pm \psi_2 \psi_3 (w_{22} w_{33} - w_{23} w_{32})}{w_{11} \mp \psi_2(w_{11}w_{22} - w_{21}w_{12}) \mp \psi_3(w_{11}w_{33} - w_{13}w_{31}) + \psi_2\psi_3 \det W}$$

where $W_{(i)}$ denote the submatrices of W obtained by deletion of i-th row and column. Without loss of generality we solved for ψ_1. Whenever the denominator of the resulting rational function becomes zero, we observe a discontinuity of the solution, such that we obtain separate branches of the bifurcation manifold. The Neimark-Sacker bifurcation condition becomes:

$$\det(J \odot J - \mathbf{1}) = -1 + (\psi_1\psi_2 M_{11} + \psi_1\psi_3 M_{22} + \psi_2\psi_3 M_{33}) + \psi_1^2\psi_2^2\psi_3^2 \det(M)$$
$$- [\psi_1^2\psi_2\psi_3 \det M_{(3)} + \psi_1\psi_2\psi_3^2 \det M_{(1)} + \psi_1\psi_2^2\psi_3 \det M_{(2)}] = 0$$

$$\text{where} \quad M := W \odot W = \begin{pmatrix} w_{22}w_{11}-w_{21}w_{12} & w_{23}w_{11}-w_{21}w_{13} & w_{23}w_{12}-w_{22}w_{13} \\ w_{32}w_{11}-w_{31}w_{12} & w_{33}w_{11}-w_{31}w_{13} & w_{33}w_{12}-w_{32}w_{13} \\ w_{32}w_{21}-w_{31}w_{22} & w_{33}w_{21}-w_{31}w_{23} & w_{33}w_{22}-w_{32}w_{23} \end{pmatrix} .$$

This condition is quadratic with respect to each ψ_i and its solution manifold splits into several branches in turn.

Note, that the test conditions as well as the bifurcation manifolds in $\boldsymbol{\psi}$-space are actually independent of the chosen activation function $\tanh$, which only influences the back transformation to the input space, which can be achieved solving (2):

$$\boldsymbol{u} = \tanh^{-1}(\bar{\boldsymbol{x}}) - W\bar{\boldsymbol{x}} \quad \text{with} \quad \bar{\boldsymbol{x}} = \boldsymbol{\psi}^{-1}(\boldsymbol{\psi}) \,. \tag{4}$$

Because $\psi_i(\bar{x}_i)$ is a quadratic function of $\bar{x}_i$, we obtain two valid preimages x_i for each $\psi_i \in (0, 1]$. Consequently the bifurcation manifolds in $\boldsymbol{\psi}$-space split into 2^n different branches in input space, leading to very complex bifurcation diagrams for large networks and making a numerical computation and a visualisation not feasible any more for $n > 3$.

In order to visualise the solution manifolds, they have to be sampled along a regular n-1-dimensional grid located in $\boldsymbol{\psi}$-space. To achieve a uniform sampling of data points, it is necessary to adapt the step size $\Delta \psi_k$ according to the gradient of the manifold at a given sampling point. Fig. 1 shows the Neimark-Sacker bifurcation manifolds of a simple three-neuron network. Due to the branching during back transformation into input space, the bifurcation diagram in input space (Fig. 1b) is much more complex than that in $\boldsymbol{\psi}$-space (Fig. 1a).

Although the abstract $\boldsymbol{\psi}$-space allows for a simpler representation of the bifurcation manifolds, it cannot be used for a separation into different regions of dynamical behaviour, because the mapping from fixed points $\bar{\boldsymbol{x}}$ or inputs $\boldsymbol{u}$ to $\boldsymbol{\psi}$-values is many-to-one – e.g. coexisting stable and unstable fixed points cannot be distinguished from a globally stable situation.

3 Bifurcation Manifolds of a cascaded 3-neuron RNN

As an example we study the dynamical properties of the cascaded 3-neuron RNN, shown in Fig. 2. It is composed from a two-neuron network, which exhibits stable oscillatory behaviour within a circular region in the u_1-u_2-plane and which projects onto a third neuron, which exhibits an hysteresis domain of two stable fixed points in an interval $[u_3^-, u_3^+]$, if the self-feedback weight $c > 1$ [Pasemann, 2002, 1993].

Due to the cascaded nature of the network, its qualitative dynamical properties can be derived without computation of the bifurcation manifolds. In fact it can be proven for general cascaded networks, that the test conditions split into the appropriate conditions of the recurrent subnetworks, such that the bifurcation manifolds in $\boldsymbol{\psi}$-space resemble those of the subnetworks [Haschke, 2003].

Hence, all neurons become oscillatory if the inputs u_1-u_2 enter the central vertical tube in the bifurcation diagram of Fig. 2, which resembles the circular bifurcation curve of the x_1-x_2 subnetwork. The saddle-node bifurcation points $u_3^\pm$ vary as a function of the average activities $\bar{x}_1, \bar{x}_2$, which in turn depend on the inputs u_1, u_2. Consequently the saddle-node bifurcation surface smoothly varies in three-dimensional input space.

While the oscillation frequency is completely determined by the oscillator subnetwork, the amplitude of the x_3-oscillation can be varied smoothly as function of
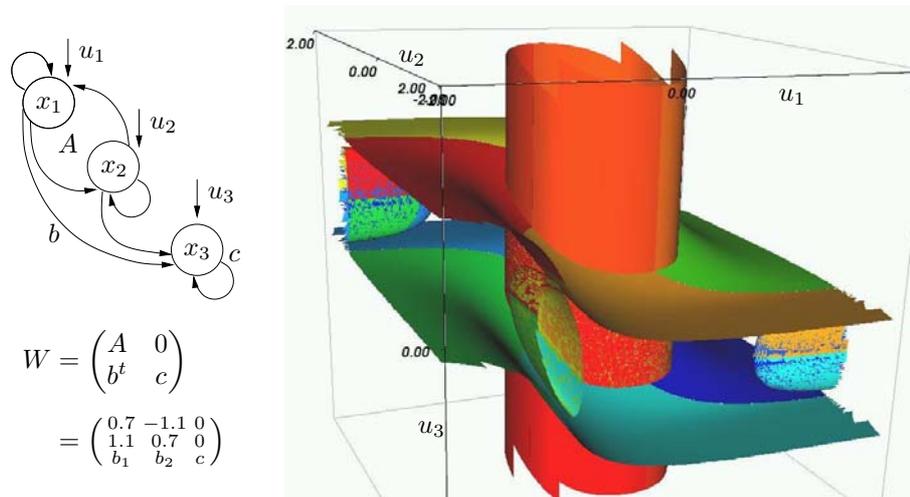
Figure 2: Bifurcation manifolds of a cascaded network, composed of an oscillatory two-neuron network which projects to a single Cusp neuron.

the input component u_3 (Fig. 3). The largest amplitudes occur, if the overall input $h = u_3 + \sum w_{3j}x_j$ becomes zero in average, i.e. varies about the point of maximal slope. In this case the external oscillatory input has the largest impact on x_3.

The hysteresis due to the Cusp bifurcation of the single neuron is preserved in the externally driven case as well: If the input u_3 is varied from negative to positive values and back we observe a switching between two stable periodic orbits. If the amplitude of the external input becomes large enough, the state x_3 continously switches between the two stable fixed-point branches of the Cusp neuron, resulting in a rectangular oscillation of maximal amplitude. Fig. 4 shows that we can generate various wave forms in dependence of b_1 ($\boldsymbol{u} = 0$ is chosen).

4   Discussion

We present analytical expressions for bifurcation manifolds in the input space of general discrete-time RNNs, which we solve for the case of three-neuron networks. Employing these expressions, we can visualise the complex partitioning of the input space into regions of different dynamical behaviour. This allows us to choose directly input control variables in order to provoke a specific dynamical behaviour. Clearly, the 3d-bifurcation manifolds of Fig. 1, 2 cannot be obtained in reasonable time by simulation and inspection of the observed time series. Hence, our new approach admits the computation of bifurcation manifolds of networks with more than two neurons.

Note, that we restrict ourselves to codim-1 bifurcations of fixed points. The whole bifurcation diagram can be more complex and may contain bifurcations of higher codimension, bifurcations of periodic points, and global bifurcations, whose corresponding manifolds cannot be computed analytically yet. Nevertheless fixed point
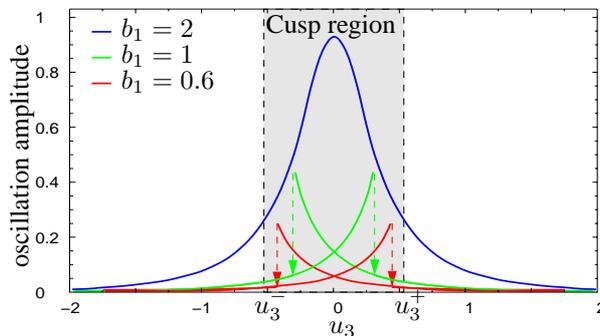
Figure 3: The oscillation amplitude of x_3 as a function of the input component u_3 and the feedforward weight b_1 ($b_2 = 0$). It can be varied smoothly from zero to a certain maximum, which depends on the weight matrix.
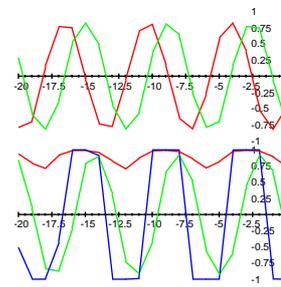
Figure 4: Time series of oscillatory neurons (above) and driven Cusp neuron (below) as functions of $b_1 \in \{1, 2, 10\}$.

bifurcations are the most frequently occurring bifurcations, bounding the parameter space corresponding to globally asymptotic behaviour.

If large networks with only a few input channels are considered, the bifurcation diagram in the high-dimensional input space has to be restricted to a low-dimensional cross section. Nevertheless the complicated structure of the bifurcation diagram persists, because it originates from the bifurcation condition involving the high-dimensional state-space of all neurons.

References

Randall D. Beer. On the dynamics of small continuous-time recurrent neural networks. *Adaptive Behaviour*, 3(4):469–509, 1995.

Robert Haschke. *Bifurcations in Discrete-Time Neural Networks – Controlling Complex Network Behaviour with Inputs*. PhD thesis, University of Bielefeld, 2003, *submitted*

Robert Haschke, Jochen J. Steil, and Helge Ritter. Controlling oscillatory behaviour of a two neuron recurrent neural network using inputs. *Proc. ICANN 2001*, 1109–1114, 2001.

Frank C. Hoppensteadt and Eugene M. Izhikevich. *Weakly Connected Neural Networks*. Springer, New York, applied mathematical sciences edition, 1997.

Yuri A. Kuznetsov. *Elements of Applied Bifurcation Theory*, volume 112 of *Applied Mathematical Sciences*. Springer-Verlag, New York, Berlin, Heidelberg, 1995.

Frank Pasemann. Dynamics of a single model neuron. *Int. Journal of Bifurcation and Chaos*, 3 (2):271–278, 1993.

Frank Pasemann. Complex dynamics and the structure of small neural networks. *Network: Computation in Neural Systems*, 13:195–216, 2002.

Peter Tiňo, Bill G. Horne, and C. Lee Giles. Attractive periodic sets in discrete-time recurrent neural networks. *Neural Computation*, 13:1379–1414, 2001.

A. Tonnelier, S. Meignen, H. Bosch, and J. Demongeot. Synchronization and desynchronization of neural oscillators. *Neural Networks*, 12(9):1213–1228, 1999.